


Performance of a low-power wide-area network based on LoRa technology: Doppler robustness, scalability, and coverage

International Journal of Distributed
Sensor Networks
2017, Vol. 13(3)
© The Author(s) 2017
DOI: 10.1177/1550147717699412
journals.sagepub.com/home/ijdsn


Juha Petäjäjärvi¹, Konstantin Mikhaylov¹, Marko Pettissalo²,
Janne Janhunen¹ and Jari Linatti¹

Abstract

The article provides an analysis and reports experimental validation of the various performance metrics of the LoRa low-power wide-area network technology. The LoRa modulation is based on chirp spread spectrum, which enables use of low-quality oscillators in the end device, and to make the synchronization faster and more reliable. Moreover, LoRa technology provides over 150 dB link budget, providing good coverage. Therefore, LoRa seems to be quite a promising option for implementing communication in many diverse Internet of Things applications. In this article, we first briefly overview the specifics of the LoRa technology and analyze the scalability of the LoRa wide-area network. Then, we introduce setups of the performance measurements. The results show that using the transmit power of 14 dBm and the highest spreading factor of 12, more than 60% of the packets are received from the distance of 30 km on water. With the same configuration, we measured the performance of LoRa communication in mobile scenarios. The presented results reveal that at around 40 km/h, the communication performance gets worse, because duration of the LoRa-modulated symbol exceeds coherence time. However, it is expected that communication link is more reliable when lower spreading factors are used.

Keywords

Internet of Things, low-power wide-area network, LoRa, mobility, performance, experiment

Date received: 6 September 2016; accepted: 18 February 2017

Academic Editor: Seong-eun Yoo

Introduction

The low-power wide-area networks (LPWANs) represent a new trend in the evolution of telecommunication designed to enable broad range of Internet of Things (IoT) applications. In contrast to the existing and perspective communication technologies (e.g. fourth generation (4G) or fifth generation (5G)), the high data rate for each device is not considered to be the most important design factor for LPWANs. Instead, the data rates in LPWANs are intentionally kept low and are traded for long communication ranges. The other critical design metric for LPWANs is the energy efficiency,

since many of end devices are expected to be powered by a battery or even with energy harvesting. Finally, the high network capacity and low hardware complexity of an end device are also important to keep the cost of a device low. Although these features inevitably limit

¹Centre for Wireless Communications, University of Oulu, Oulu, Finland
²Nokia, Oulu, Finland

Corresponding author:

Juha Petäjäjärvi, Centre for Wireless Communications, University of Oulu, Erkki Kooiso-Kanttilan Katu 3, 90570 Oulu, Finland.
Email: juha.petajarvi@oulu.fi



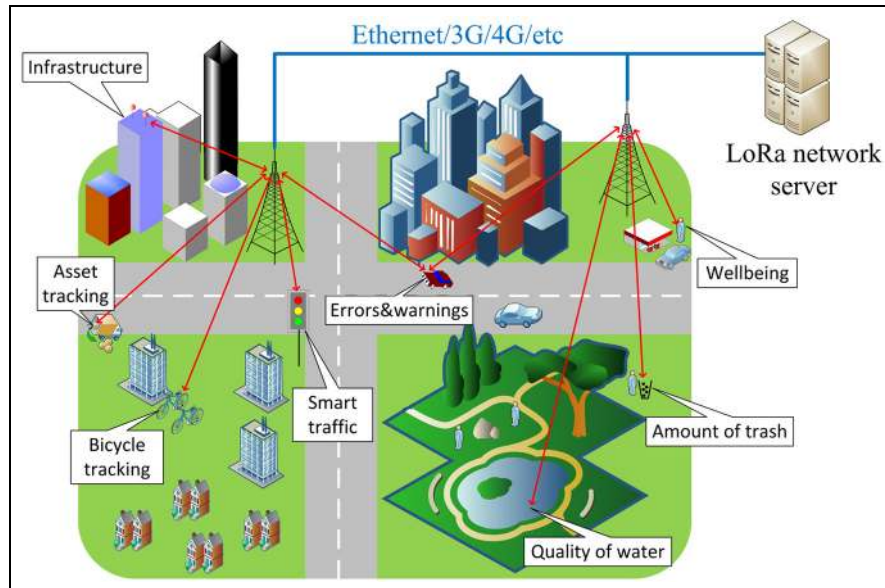


Figure 1. In the future IoT applications, infrastructure, people, trash bins, bicycles, cars, etc. are possibly monitored with LPWAN technologies, such as LoRa.

the range of LPWAN applications (by excluding, for example, the ones requiring data-hungry media streaming), the number of applications which will benefit from using these technologies is really tremendous. To give few practical examples, the LPWANs suit quite well the requirements of, for example, smart metering applications (e.g. gas, water, electricity, and garbage), civil engineering and infrastructure monitoring (e.g. tunnels, bridges, and buildings), and environment conditions (pollution and climate). Besides, LPWANs can be employed for tracking of vehicles (e.g. cars, bicycles, and motorcycles), and monitoring peoples' well-being. Figure 1 depicts few potential IoT example use cases for LPWANs.

Although the LPWANs have much in common with the traditional wireless sensor networks (WSNs), there are few critical differences, especially when this comes to the requirements for networks and end devices. The first and the major difference is that unlike the traditional WSNs which usually employ mesh topology, the state-of-the-art LPWAN technologies require setting up the gateways (referred to as concentrators or base stations, depending on the terminology) to serve an end device. The end devices communicate directly to one or more gateways as shown in Figure 1. Depending on the technology, the coverage area of a single gateway may range from hundreds of meters to tens of kilometers and may include thousands or even millions of end devices.

Over the last few years, LPWAN technologies have drawn a lot of attention in the media due to the large investments from private sector. Today, several competing technology providers are actively trying to gain

ground of the global markets. For example, Sigfox¹ acts as both a service and a technology provider for LPWAN and covers multiple countries of the central Europe and many countries are under roll out such as USA, Australia and Finland. The second major player is the LoRa Alliance,² which was officially established in 2015, and which stands after the LoRa technology. Also, the start of deployment of the first Weightless networks based on the technology handled by the Weightless special interest group³ has been recently announced.⁴ In addition to these LPWAN technologies, the traditional telecom industry is also driving toward IoT. The long-term evolution for machine-to-machine (LTE-M) and the narrowband IoT (NB-IoT) have recently been shaped in the Release 13 standard by the 3rd Generation Partnership Project (3GPP).⁵ This will bring further optimizations for device cost, battery lifetime, and coverage. Namely, reduced transmit power in addition to power spectral density improvement and allowing, for example, higher error rate or longer acquisition time are expected to enable enhanced coverage and energy efficiency. Also part of Release 13, Global System for Mobile Communications (GSM)–Enhanced Data rates for GSM Evolution (EDGE) radio access network will be standardized as an Extended Coverage GSM solution⁶ that supports over 10 km range. In general, future cellular IoT can be seen having benefits from large number of vendors and operators. Moreover, there are numerous technologies featuring similar characteristics such as WAVIoT, Nwave, Telensa, Cyan's Cynet, Accellus, SilverSpring's Starfish, and Ingenu/On-Ramp.⁷

In this article, we focus on the performance of the LPWAN and, namely, the LoRa radio technology. The major contribution of this article includes three aspects. First, we analyze the performance of LoRa modulation for mobile use case when the end device's radio signal is affected by Doppler. Second, we characterize the capacity of a LoRa wide-area network (LoRaWAN) for several illustrative use-case scenarios. Third, we report results of the field trial measurements conducted using commercial LoRa end devices. The presented results provide an insight on the real-life performance of the technology.

Since the LPWAN concept in general and the LoRa technology in particular are quite new, they have not got much of attention from the academic community yet. Overview of nine different technologies has been done in Sanchez-Iborra and Cano,⁸ while an overview focusing specifically on LoRa and Sigfox is introduced in Nolan et al.⁹ In Reynders et al.,¹⁰ the performance of the LoRa-like spread spectrum and Sigfox-like ultra narrowband (UNB) technologies are compared under interference. The simulation results revealed that for the applications which require higher throughput at relatively short range, the spread spectrum approach suits better than UNB. For the applications requiring longer range, the UNB systems outperform the spread spectrum ones. The quality of service of the LoRa was measured with fixed 3-km range in Petrić et al.¹¹ Augustin et al.¹² focused on the LoRa technology by introducing the network architecture, physical (PHY), and medium access control (MAC) layers. The LoRa outdoor coverage was addressed in Petäjälä et al.¹³ We used the lowest bandwidth (i.e. 125 kHz) and the maximum spreading factor (SF) possible (i.e. 12) in our experiments. With these settings, we observed the communication ranges of over 15 km on ground and almost 30 km on water with 14 dBm transmit power. We measured indoor coverage at the University of Oulu premises with the same settings in Petäjälä et al.¹⁴ The results showed that the entire campus area can be covered with an average success delivery ratio of almost 97%. Even from a cellar, almost 95% of the packets were delivered successfully. We have also studied the scalability and capacity of the LoRa technology in Mikhaylov et al.¹⁵ In Wendt et al.,¹⁶ the performance and indoor through-obstacle penetration of the LoRa-like modulation in the 2.4 GHz frequency band are studied. Although the results of this study require adaptation (since LoRaWAN operates exclusively in sub-GHz bands), some of the witnessed effects and made conclusions can be valid also for the lower frequency bands. This article introduces novel findings which are tied together with results from our previous works introduced in Petäjälä et al.¹³ and Mikhaylov et al.¹⁵ in order to get a more comprehensive picture of the LoRa technology and its application possibilities.

This article is organized as follows. In section "The LoRa technology," we provide a brief introduction and overview of the LoRa technology. In section "Analysis of the LoRaWAN performance," we give the theoretical analysis of the performance of LoRa modulation and LoRaWAN performance, namely, the robustness against Doppler effect, throughput, and network capacity. In section "Experimental measurements and results," we present the results of the real-life measurements illustrating the practical performance of the technology. Finally, in section "Discussion," we conclude the article with discussion about the obtained results.

The LoRa technology

Technically, the LoRaWAN specification¹⁷ includes three major components, namely, the PHY layer, the link layer, and the network architecture.

PHY layer

The communication between an end device and a gateway is handled in the different sub-GHz frequency bands depending on the local frequency regulations. In this article, we address specifically the operation in the EU industrial, scientific, and medical (ISM) 868 MHz band. For this band, the LoRaWAN specification enables eight PHY options. Six of them are based on LoRa modulation with SF between 7 and 12 and with bandwidth of 125 kHz. One option is based on 250 kHz bandwidth and SF of 7 LoRa modulation, and the eight option is Gaussian frequency-shift keying (GFSK) with 50 kbps data rate.

The LoRa modulation is based on chirp spread spectrum (CSS) scheme that uses wideband linear frequency-modulated pulses whose frequency decreases or increases over a specific amount of time based on the encoded information.¹⁸ The use of high bandwidth-time product makes the radio signals resistant against in-band and out-of-band interferences, while the use of sufficiently broadband chirps enables to improve robustness against multipath fading.¹⁹ This results in the maximum link budget of about 157 dB, which enables to achieve long communication ranges or to reduce the transmit power, thus saving the energy of the end devices. The used modulation scheme is also expected to help mitigating the Doppler effect. Furthermore, LoRa modulation includes a cyclic error-correcting scheme, which improves the communication robustness by adding redundancy.¹⁹ To improve the spectral efficiency and increase the network capacity, LoRa modulation features six different data rates resulting from orthogonal SF codes. This enables multiple access method on the same channel¹⁹ without degrading the communication performance.

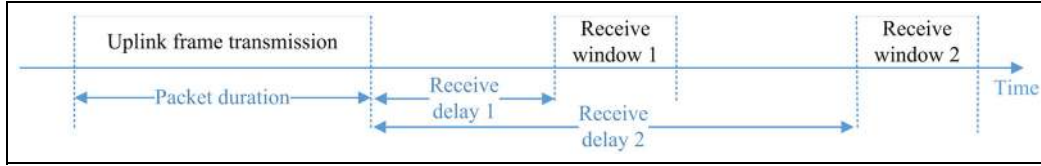


Figure 2. Communication phases of a class A LoRaWAN device.

Link layer

The MAC protocol in 1.0 version of the LoRaWAN specification¹⁷ defines that end devices access the medium for transmitting their packets in a pure ALOHA fashion. The MAC layer also defines three options for scheduling the receive window slots for downlink communication, which are named as classes A, B, and C. The end device must have a support for class A, but support for classes B and C is optional. As shown in Figure 2, two receive windows are opened after each uplink transmission in class A. In addition to the two receive slots after each uplink frame, in class B, an extra receive window is open at scheduled times. To have a support for class B, gateway periodically transmits beacon packets for providing the time reference and maintaining the synchronization. Class C devices stay in receive mode unless they are transmitting. In this article, we consider explicitly the end devices of class A.

Network architecture

The LoRaWANs typically employ a star-of-stars topology where the gateways relay data messages between the end devices and the network server as shown in Figure 1. The important feature of the LoRa technology, named adaptive data rate (ADR), resides in the network server. The ADR allows adapting and optimizing the data rate for the static end devices. Mobile end devices should use fixed data rate since mobility can cause significant temporal variations for the radio channel characteristics.¹⁷ However, in many mobile applications, the end devices are actually static most of the time that makes possible for them to request the network server to optimize data rate. For example, an end device mounted to a trash bin's lid is moved when trashes are put there or it is being emptied, but remains static rest of the time. Another important component of the network server is a mechanism used to filter out the redundant packets. Since the technology does not employ any handover method, a single packet transmitted by an end device may get received by several gateways, each of which will forward such a packet to the server. Although this technical solution inevitably

introduces redundancy in respect to the backbone communication, it enables to eliminate the handover-related signaling, thus bringing some energy savings. The network server is also responsible for security, diagnostics, and acknowledgements.²⁰

Analysis of the LoRaWAN performance

In this section, we discuss how robust the LoRa technology is against Doppler effect. Also, the throughput and the network capacity of the LoRaWAN are analyzed and discussed.

Doppler effect

It is well known that when a source of a wave is moving relative to an observer, the observer receives a frequency which differs from the one radiated. The difference depends on the source's movement direction and velocity. When this comes to wireless communications, this effect may hamper the correct reception of the signal.

Let's assume that a chirp signal is transmitted from a moving end device, which is given by²¹

$$s(t) = \begin{cases} A(t) \cos\left[(\omega_0 + \omega_D)t + \frac{\mu t^2}{2}\right], & -T/2 < t < T/2 \\ 0, & \text{elsewhere} \end{cases} \quad (1)$$

where A is the amplitude of the signal, ω_0 is the angular carrier frequency, ω_D is the angular frequency shift caused by Doppler effect, t is time, μ is the chirp rate, and T is the duration of the chirp. This CSS signal is called up-chirp when frequency linearly increases ($\mu > 0$) and down-chirp when frequency decreases ($\mu < 0$).

The frequency shift due to the Doppler effect causes the autocorrelation peak on the receiver to shift in time. The time shift can be calculated as ω_D/μ .²¹ If the chirp rate is large, the time shift is so small that it can be neglected. This makes CSS to perform well in the presence of Doppler effect. However, the LoRa technology provides long-range communication link at the cost of data rate. This inevitably has an impact on the chirp

rate. With a low chirp rate, the time shift is increased, which makes receiving packets correctly more difficult.

Another approach to analyze performance of the LoRa technology is to compare coherence time (T_c)

$$\begin{aligned} T_{\text{LoRa}} &= T_{\text{preamble}} + T_{\text{packet}} \\ &= \frac{1}{R_s} \left(n_{\text{preamble}} + \left(SW + \max \left(\text{ceil} \left[\frac{8PL - 4SF + 28 + 16CRC - 20IH}{4(SF - 2DE)} \right] (CR + 4), 0 \right) \right) \right) \end{aligned} \quad (4)$$

and symbol time (T_s). Coherence time is inversely proportional to Doppler shift as

$$T_c = \frac{2\pi}{\omega_D} \quad (2)$$

If $T_s > T_c$, fast fading occurs due to the Doppler effect, which leads into signal distortion.²² Symbol time in LoRa modulation can be calculated as¹⁹

$$T_s = \frac{2^{SF}}{BW} \quad (3)$$

where SF is the spreading factor and BW is the bandwidth. As can be noticed from equation (3), T_s doubles when SF is increased by one, given that the bandwidth does not change.

In order to see when fast fading occurs, coherence time with center frequency of 868 MHz at different velocities is shown in Figure 3 along with periods of LoRa-modulated symbols with different SFs and bandwidths. When the velocity is under 38 km/h, the T_c is larger than T_s with shown SFs. At 38 and 76 km/h, T_c and T_s curves with $SF = 12$ and $SF = 11$ cross, respectively. Therefore, the LoRa technology might experience packet losses at relatively low velocities with these SFs. Lower SFs can tolerate higher speeds.

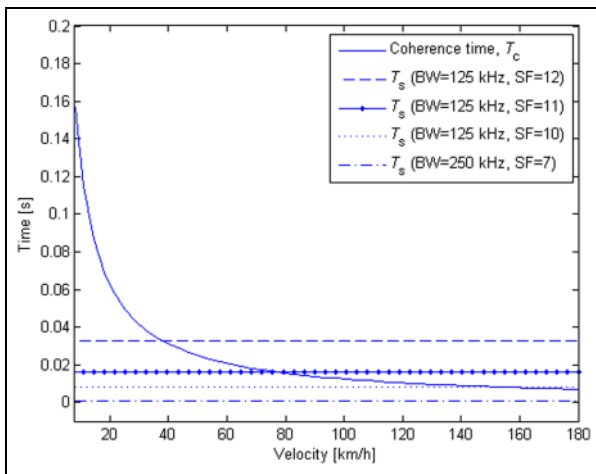


Figure 3. Comparison of the coherence time and symbol times for LoRa signals with different spreading factors.

End device data rate

According to Semtech,²³ the duration of a LoRaWAN frame is composed of a preamble and the actual packet payload and is given by

for LoRa modulation and by

$$\begin{aligned} T_{\text{GFSK}} &= T_{\text{preamble}} + T_{\text{packet}} \\ &= \frac{8}{R_{\text{GFSK}}} (L_{\text{preamble}} + SW + PL + 2CRC) \end{aligned} \quad (5)$$

for GFSK, where R_s is the symbol rate, $n_{\text{preamble}} = 12.15$ is the number of preamble symbols for a LoRa-modulated packet, $L_{\text{preamble}} = 5$ bytes in GFSK, SW is the length of synchronization word ($SW = 1$ byte for LoRa and 3 bytes for GFSK), PL is the number of payload bytes, SF is the spreading factor, CRC specifies the presence of payload cyclic redundancy check. $CRC = 1$ when enabled and zero otherwise. IH indicates the operation mode. $IH = 0$ in explicit mode and $IH = 1$ in implicit mode. For LoRa modulation, DE stands for data rate optimization which introduces overhead to increase robustness to reference frequency variations over the timescale of the LoRa frame (mandatory for SFs exceeding 10 at 125 kHz bandwidth). $DE = 1$ when the optimization is enabled and $DE = 0$ otherwise. CR is the coding rate and ranges from 1 to 4. R_{GFSK} is GFSK-modulated data rate (50 kbps). \max denotes the function returning the maximum of the two arguments in the brackets separated by the comma, and ceil designates the function mapping a real number argument to the smallest following integer.

Based on the frame formats defined in Semtech,²³ the length of the PHY layer payload in bytes is given by

$$\begin{aligned} PL &= MHDR + MAC_{\text{payload}} + MIC \\ &= MHDR + FHDR_{\text{ADDR}} + FHDR_{\text{CTRL}} \\ &\quad + FHDR_{\text{CNT}} + FHDR_{\text{OPTS}} + F_{\text{port}} \\ &\quad + FRM_{\text{payload}} + MIC \\ &= 12 + FHDR_{\text{OPTS}} + F_{\text{port}} + FRM_{\text{payload}} \end{aligned} \quad (6)$$

where $MHDR = 1$ is the length of MAC header; $FHDR_{\text{ADDR}} = 4$ is the length of the frame header (FHDR) address field; $FHDR_{\text{CTRL}} = 1$ and $FHDR_{\text{CNT}} = 2$ are the lengths of the FHDR's frame control and frame counter fields, respectively; $FHDR_{\text{OPTS}}$ is the optional FHDR field's length; $F_{\text{port}} = 1$ is the port identifier for an application specific; and $MIC = 4$ is the message integrity code.

The payload's maximum length depends on the used transmission mode as shown in the five leftmost columns of Table 1. The frame duration values presented in the four rightmost columns were calculated using equations (3)–(5) for FRM_{payload} equal to 0 (shortest frame) and the maximum possible value (longest frame). As one can see from the presented results, the transmission of a single frame using LoRa modulation with high SFs may take more than a second.

Based on these results, the maximum application layer throughput under the different duty cycle restrictions imposed by the European frequency regulations²⁴ for various 868 MHz sub-bands is summarized in Table 2. Note that for GFSK and 10% end device duty cycle, the throughput is restricted by the need of opening the receive windows after uplink transmission, rather than the frequency regulations. Nonetheless, one can clearly see that the potential absolute uplink application layer data rate available to a LoRaWAN end device does not exceed 2 kbps even under error-free communication.

Scalability and network capacity

LoRa modulation technique enables long-range communication, which inevitably raises the question of how many end devices can be served by a single LoRaWAN gateway. To answer this question, we analyzed the maximum LoRaWAN cell capacity for several characteristic M2M communication use cases derived from IEEE 802.16 Broadband Wireless Access Working Group.²⁵ The results presented in Table 3 are given for three different network settings with unacknowledged uplink transmission. In the first case, three obligatory 125-kHz LoRa-modulated channels were considered, and six 125-kHz LoRa channels in the second case. In the third case, six 125-kHz LoRa channels, one 250-kHz LoRa, and one GFSK channel were investigated. The results were obtained using equations (3)–(5). Since LoRa modulation uses orthogonal SFs,¹⁹ it is assumed that all the SFs can be used at the same time in each 125 kHz channel. The results of the maximum theoretical capacity under perfect synchronization and scheduling of the end devices are given in Table 3. However, the end devices are assumed to access the channel randomly in a pure ALOHA fashion as described in the LoRaWAN specification. Utilizing the pure ALOHA for accessing the channel can be justified if to account for the well-known hidden-node problem and for the push for omitting listen-before-talk (LBT) phase for enabling energy savings. It is well known²⁶ that the optimal capacity for ALOHA is $0.5/e$ times the maximum, which is shown in the rightmost column of Table 3.

The presented results show that for infrequent transmissions (e.g. once a day—see house appliance case in Table 3) of short messages, a single LoRaWAN

Table 1. LoRaWAN data rate settings and frame characteristics.

Modulation	SF	Bandwidth (kHz)	Maximum MAC _{payload} size (bytes)	Maximum FRM _{payload} size ^a (bytes)	Shortest downlink frame duration (s)	Longest downlink frame duration (s)	Shortest uplink frame duration (s)	Longest uplink frame duration (s)
LoRa	12	125	59	51	0.991	2.793	1.155	2.793
LoRa	11	125	59	51	0.578	1.479	0.578	1.561
LoRa	10	125	59	51	0.289	0.698	0.289	0.698
LoRa	9	125	123	115	0.144	0.677	0.144	0.677
LoRa	8	125	250	242	0.072	0.697	0.082	0.707
LoRa	7	125	250	242	0.041	0.394	0.041	0.400
LoRa	7	250	250	242	0.021	0.197	0.021	0.200
GFSK	–	150	250	242	0.0032	0.0421	0.0035	0.0424

SF: spreading factor; GFSK: Gaussian frequency-shift keying.

^aGiven that $FHDR_{\text{OPFS}} = 0$.

Table 2. Maximum throughput per LoRaWAN end device per channel.

Modulation	Spreading factor	Bandwidth (kHz)	Maximum application throughput per channel (bps)	Maximum application layer throughput per end device per channel (bps)		
				10% duty cycle ^a	1% duty cycle ^b	0.1% duty cycle ^c
LoRa	12	125	146.1	14.61	1.46	0.15
LoRa	11	125	261.4	26.14	2.61	0.26
LoRa	10	125	584.2	58.42	5.84	0.58
LoRa	9	125	1359.2	135.92	13.59	1.36
LoRa	8	125	2738.1	273.81	27.38	2.74
LoRa	7	125	4844.7	484.47	48.45	4.84
LoRa	7	250	9689.3	968.93	96.89	9.69
GFSK	–	150	45,660.4	1851.6 ^d	456.6	45.66

^a869.400–869.650 MHz with up to 500 mWV effective radiated power (ERP).

^b868.000–868.600 and 869.700–870.000 MHz and with up to 25 mWV ERP.

^c868.700–869.200 MHz bands with up to 25 mWV ERP.

^dDue to the need for opening receive windows after each frame, the maximum possible end device duty cycle is 4.1% (transmission acknowledged in the first receive slot using the shortest packet transmitted with the same settings).

Table 3. Capacity of a LoRaWAN cell.

Scenario	Average message period	Average message size (byte)	Network configuration			No. of end devices per cell	
			No. of 125-kHz LoRa channels	No. of 250-kHz LoRa channels	No. of GFSK channels	Maximum under perfect synchronization	Optimal for pure ALOHA access
Roadway signs	30 s	1	3	0	0	4017	739
			6	0	0	8034	1478
			6	1	1	15,928	2930
Traffic sensors	60 s	1	3	0	0	8187	1506
			6	0	0	16,374	3012
			6	1	1	34,715	6385
Elderly sensors	60 s	127 ^a	3	0	0	1419	261
			3	0	0	3024	556
			3	0	0	6027	1109
House appliances	1 day	8	3	0	0	9,722,253	1,788,309
			6	0	0	19,444,506	3,576,617
			6	1	1	39,778,804	7,316,902
Credit machine in a shop	30 min	24	3	0	0	142,167	26,150
			6	0	0	284,334	52,300
			6	1	1	568,140	104,504
Home security	10 min	20	3	0	0	52,569	9670
			6	0	0	105,138	19,339
			6	1	1	208,775	38,402
Smart meters	2.5 h	2017 ^a	3	0	0	16,440	3024
			6	0	0	434,592	79,939
			6	1	1	889,697	163,651

LoRaWAN: LoRa wide-area network; GFSK: Gaussian frequency-shift keying.

^aPackets fragmented into the packets with the maximum permitted payload for particular data rate.

gateway can support up to few millions end devices. For more frequent transmissions (e.g. roadway signs and traffic sensors in Table 3 having 30 and 60 s report periods, respectively), hundreds to thousands of end devices can operate in a cell. Using the data about the density of the end devices for the discussed scenarios,

which was reported in IEEE 802.16 Broadband Wireless Access Working Group,²⁵ and assuming that the whole radio channel is used exclusively by the target application, in Table 4, we analyze how dense the gateways have to be placed. The reported results reveal that if for the frequently reporting devices (e.g. traffic

Table 4. Network density.

Scenario ^a	Network configuration			Average density of devices		Radius of cell service area (km) ^b	
	No. of 125-kHz LoRa channels	No. of 250-kHz LoRa channels	No. of GFSK channels	Urban scenario, devices/km ^b	Suburban scenario, devices/km ^b	Urban scenario	Suburban scenario
Roadway signs	3	0	0	316	943	0.86	0.50
	6	0	0	316	943	1.2	0.71
	6	1	1	316	943	1.8	1.0
Traffic sensors	3	0	0	38,500	14,800	5.6	2.0
	6	0	0	38,500	14,800	8.0	2.9
	6	1	1	38,500	14,800	11.6	4.2
Elderly sensors	3	0	0	209	23.1	3.8	19.6
	3	0	0	209	23.1	5.4	27.7
	6	1	1	209	23.1	7.8	Over 30
House appliances	3	0	0	3850	1480	6.3	19.0
	6	0	0	3850	1480	8.9	26.8
	6	1	1	3850	1480	12.6	Over 30
Credit machine in a shop	3	0	0	385	148	0.89	1.4
	6	0	0	385	148	1.3	2.0
	6	1	1	385	148	1.8	2.9
Home security	3	0	0	11,500	4440	0.46	0.24
	6	0	0	11,500	4440	0.68	0.35
	6	1	1	11,500	4440	0.96	0.49
Smart meters	3	0	0	316	943	0.29	0.81
	6	0	0	316	943	1.5	4.1
	6	1	1	316	943	2.1	5.9

GFSK: Gaussian frequency-shift keying.

^aBased on IEEE 802.16 Broadband Wireless Access Working Group.²⁵

^bBased on the sensitivities of a gateway specified in Semtech²³ and LoRa channel attenuation model for suburban areas reported in Petäjäjärvi et al.¹³ Further details are reported in Mikhaylov et al.¹⁵

sensors), the gateways need to be placed at a distance of units of kilometers, and for the rarely reporting end devices, the gateways can be placed dozens of kilometers apart. Nonetheless, a significant issue related to the LoRaWAN scalability potential is the distribution of the end devices over the coverage area. As one can see from Table 2, almost the half of the total throughput for the third network configuration is provided by the GFSK channel, which is shown to have the maximum communication range of less than 1.5 km.²⁷ This means that most of the end devices, and especially the ones requiring high throughput, have to be grouped in the direct vicinity of the gateway. The other issue which somewhat limits the scalability of a LoRaWAN is the downlink communication. Note that the LoRaWAN gateways are subject to the duty cycle restrictions similar to the ones imposed on the end devices (refer to Table 2). First of all, this means that the amount of downlink traffic needs to be rather small and the downlink packets may experience long transmission delays due to frequency access back-offs. Second, this calls for very careful use of the acknowledgements by the gateways since they inevitably reduce the on-air time available for actual data transfers.

Experimental measurements and results

In order to assess the practical capabilities and constraints of the LoRa technology, three practical experiments were conducted. In the first two setups, the performance of the real-life LoRa end devices under Doppler frequency shift was investigated. Specifically, we aimed at measuring the performance with SF = 12 at velocities that we expected to be difficult for the LoRa technology, that is, over 38 km/h (as discussed in section “Doppler effect”). In the first setup, we mounted the end device to a lathe installed in the laboratory environment, which was used to generate different angular velocities for the end device. In the second setup, the end device was mounted to a car that was driven via a motorway passing the gateway. In the third setup, the end device was also mounted to the car, but this time the end device was used to measure the outdoor coverage.

The experimental measurements had a set of common setup parameters. For the experiments, we have deployed a single LoRa-enabled cell. The commercial LoRa gateway (Kerlink’s LoRa IoT) was installed at the premises of the Faculty of Information Technology

Table 5. Frequency channels used in the tests and the respective EU regulations.

f_c (MHz)	Maximum effective radiated power ²⁴ (dBm)	Spectrum access ²⁴
868.100	14	1% or LBT AFA
868.300	14	1% or LBT AFA
868.500	14	1% or LBT AFA
868.850	14	0.1% or LBT AFA
869.050	14	0.1% or LBT AFA
869.525	27	10% or LBT AFA

LBT AFA: listen-before-talk adaptive frequency agility.

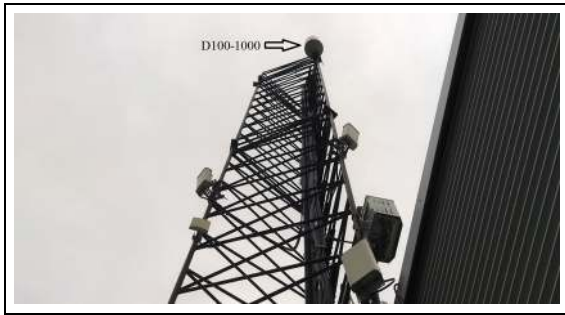


Figure 4. LoRa base station's antenna attached to the University of Oulu antenna tower.

and Electrical Engineering (ITEE) of the University of Oulu. The gateway's antenna (D100-1000 antenna from Aerial²⁸) providing 2 dBi gain over the band from 100 MHz to 1 GHz was located at the antenna tower at a height of around 24 m from sea level as depicted in Figure 4.

We used LoRa end devices that are equipped with a Semtech SX1272 transceiver²³ and have a printed circuit board Planar-F antenna. The devices were programmed with firmware version 3.1. Besides the SX1272 transceiver, each end device contained a global positioning system (GPS) signal receiver and a set of sensors. During the measurements, the end devices were powered by 9-V batteries. The end devices were configured to periodically report their sensor data and GPS coordinates to the gateway, which forwarded the packets to the network server. Each packet contained an increasing sequence number which was used for calculating the packet delivery rate. No mechanisms for over-the-air delivery control or automatic retransmissions were enabled.

The end device and the gateway were configured to use the six frequency channels summarized along with the respective requirements from the European frequency-use regulations in Table 5. The end devices were operating as class A devices and used the constant transmit power of 14 dBm (25 mW), which is the maximum allowed for all the used sub-bands. The maximum transmit power of the end device operating in

869.400–869.650 MHz band can be increased to 20 dBm (100 mW), which enables getting even longer communication ranges. Note that each end device automatically counts its own on-air time for each radio channel and restricts the transmission following the imposed restrictions. The ADR was not used because in all measurement cases the end device was mobile most of the time.

The collection of data was greatly hampered by the long transmission times and low end device duty cycles prescribed by the frequency regulations.²⁴ Even though we have configured the end devices to report their data with a period of 5 s, during the experiments, less than five packets per minute were transmitted in average. To give a practical example, the period of packet transmission for LoRa is given by

$$T_{\text{pkt}} = \frac{1}{\sum_{i=1}^{n_{\text{channel}}} \frac{dc(i)}{T_{\text{LoRa}}}} \quad (7)$$

where n_{channel} is the number of the used frequency channels (see Table 5), dc is the duty cycle regulation for a particular channel i , and T_{LoRa} is the packet's duration. For example, for the 10 bytes payload with $\text{SF} = 12$ (which corresponds to packet duration of 1.483 s) and the six channels listed in Table 5, the resulting packet period is around 12 s. The packets with maximum payload (i.e. 51 bytes) while using the same set of channels will have a period of about 23 s.

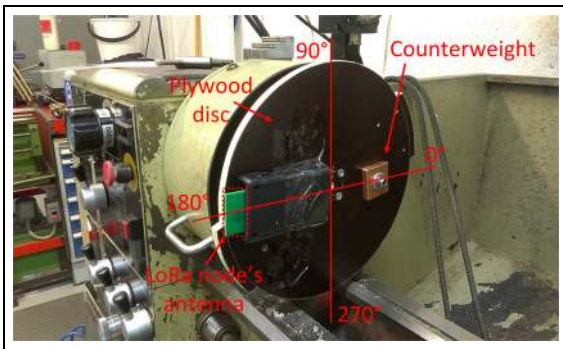
Angular velocity

We used a lathe to rotate the LoRa end device which was set to spin at different angular velocities in order to evaluate the performance of the LoRa technology under Doppler shift. The end device was mounted on a disk made of plywood that was fastened to the lathe as shown in Figure 5. A counterweight was attached opposite to the end device to prevent the undesired vibration of the disk. During the measurements the end device traveled the circular path and had angular velocity of

Table 6. RPM values used during the measurements and respective angular and linear velocities.

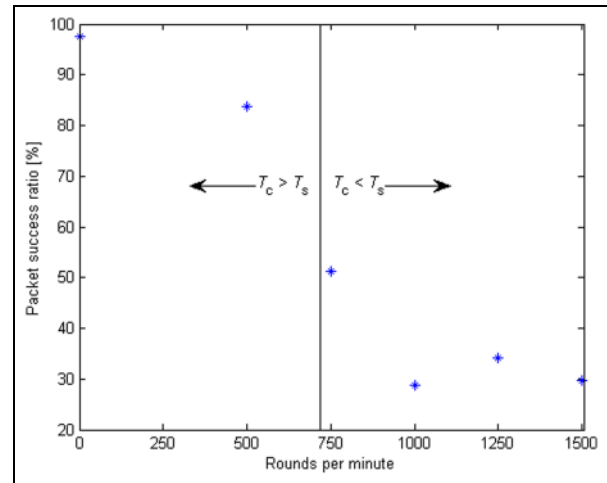
Rounds per minute	Angular velocity, rad/s	Linear velocity, m/s (km/h)	Traveled distance during T_s (d_s), m	d_s to circumference ratio, %
500	52.36	7.36 (26.49)	0.24	27.3
750	78.54	11.00 (39.60)	0.36	40.9
1000	104.72	14.67 (52.78)	0.48	54.6
1250	130.90	18.33 (65.99)	0.60	68.0
1500	157.08	21.99 (79.16)	0.72	82.0

RPM: rounds per minute.

**Figure 5.** The reference measurement setup for angular velocity experiments (node is at 180°).

$$\omega = \frac{2\pi \times RPM}{60} \quad (8)$$

where RPM stands for rounds per minute, which is the rotation speed generated by the lathe. The linear velocity can be calculated by multiplying angular velocity with radius. The radius (0.14 m) was measured from the axis of rotation to the center of the end device's antenna. Table 6 reveals the RPM values set in the measurements and the respective angular and linear velocities. The table also gives the end device's traveling distance during single LoRa (SF = 12, 125 kHz bandwidth) symbol time (T_s) and its ratio to circumference. As one can see, even for the highest RPM value (i.e. 1500 RPM), the end device does not make a full turn during T_s . This means that two scenarios can occur. In the former one, the end device moves toward the gateway until it passes by the closest point and then starts moving away from the gateway. This scenario somewhat correlates to the case when a car passes by the gateway and starts moving away. In the latter scenario, the end device moves away from the gateway and after reaching the furthest point starts approaching the gateway. The second scenario may not be so common in other circumstances. Note that in practice, the very similar behavior to the tested one may be witnessed, for example, for a wireless sensor inside a car's tire or a device attached to the shaft. The lathe used in

**Figure 6.** Packet success ratio at different angular velocities.

experiments was located at the University of Oulu workshop at a distance of approximately 75 m from the gateway. Note that the workshop environment was sufficiently challenging from the point of radio signal propagation due to presence of numerous metalwork machines, the mesh nets attached to the ceiling, the concrete walls, and shock-proof windows blocking the signal's path.

It is obvious that the end device's antenna's radiation pattern in respect to the gateway was constantly changing during the measurements. This should cause some degradation in the signal level since the antenna's radiation pattern is not omnidirectional.²⁹ This was taken into account by making a series of reference measurements with the static end device placed at different angles (namely, 0°, 90°, 180° and 270° measured with respect to the ground level). To give an example, Figure 6 illustrates the end device at 180°. Table 7 shows the packet success ratio during the reference measurements. The total measured packet success rate was 97.5% with average received signal strength of -84.9 dBm.

After the reference measurements, the lathe was set to rotate at different RPMs. For each RPM, the end device transmitted around 300 packets and then the

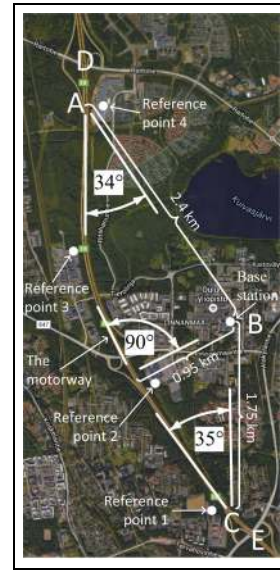
Table 7. Results of the reference measurements for angular velocity experiments.

Angle (°)	No. of transmitted packets	No. of received packets	Success ratio (%)	Average received signal strength (dBm)
0	386	376	97.4	-87.6
90	322	316	98.1	-81.6
180	377	367	97.4	-78.7
270	325	316	97.2	-81.2
Total	1410	1375	97.5	-84.9

RPM was changed. The measurements were divided into three days and the results for each day are shown in Table 8. There are two things that need to be highlighted from the results. First, the reliability of the communication decreases dramatically when the spinning speed exceeds 750 RPM. Second, there is a large variance in success rate between different days even for the same RPM values. The latter is partly explained with the fact that the number of transmitted packets is low. The other possible reasons include the variations of the environment (including the locations between the workshop and the gateway, which cannot be controlled by the authors) and the possible interferences from other systems. Note that the average received signal strength indicator (RSSI) for the rotating end device appears to be slightly lower than the one witnessed during the reference measurements, but still it is significantly higher than the sensitivity of the gateway (-137 dBm). Figure 6 depicts the effect of the angular velocities on the cumulative success rate for all the packets transmitted in 3 days. The threshold where the coherence time (T_c) becomes larger than symbol time (T_s) is also given for the reference. The experimental results seem to follow the theory even though the number of packets can be considered as too low to be statistically reliable. Nonetheless, it is pretty hard to draw any quantitative conclusions based on these results other than the one that at angular velocities higher than 78 rad/s (750 RPM in this case), the LoRa communication with SF = 12 and 125 kHz bandwidth becomes less reliable.

Linear velocity

For measuring the effect of the linear velocity, the end device was mounted on the dash board of a car, which was driven back and forth along the motorway located few kilometers away from the gateway. The maximum speed limitation on the motorway is 100 km/h. The map illustrating the position of the gateway (point B) and the part of motorway (A–C) used for testing is presented in Figure 7. Note that the motorway does not pass by the gateway in a direct angle, thus the velocity of the car relative to the gateway is lower than the

**Figure 7.** The map of the motorway and BS location during linear velocity experiments.

actual velocity of the car. The instantaneous frequency observed by the gateway is given by

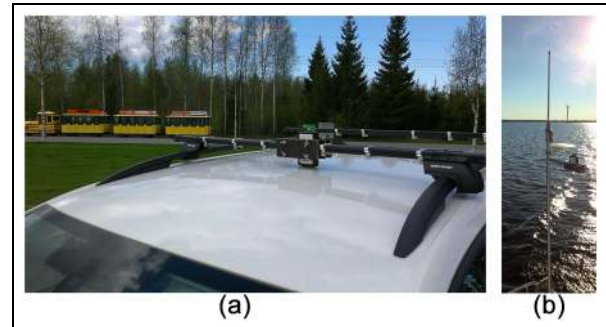
$$f_{BS} = \frac{f_c c}{c + v_{\text{end device}} \cos(\alpha)} \quad (9)$$

where f_c is the center frequency of the transmitted packet, c is the speed of wave, $v_{\text{end device}}$ is the velocity of the car and α is the angle between the car's movement direction and the direction toward gateway. The absolute relative velocity has its maximum of approximately 82.9 km/h at 34° and minimum of 0 km/h at 90° . Also, the map illustrates the position of the four reference measurement points in which the car was parked and which were used to assess the communication performance in the absence of the Doppler. Since it is illegal to park the car on the motorway directly, the reference points were chosen as close to the motorway as possible. Note that the car was turned around at road junctions D and E, nonetheless only the packets sent between points A and C were analyzed (filtering was done based on packet's GPS coordinates).

Table 8. Packet success rate at different angular velocities.

RPM	Day 1					Day 2					Day 3					
	No. of transmitted packets	No. of received packets	Success rate (%)	Average RSSI (dBm)	No. of transmitted packets	No. of received packets	Success rate (%)	Average RSSI (dBm)	No. of transmitted packets	No. of received packets	Success rate (%)	Average RSSI (dBm)	No. of transmitted packets	No. of received packets	Success rate (%)	Average RSSI (dBm)
	500	297	254	85.5	-86.9	300	257	85.7	-86.2	299	240	80.3	-85.5	299	240	80.3
750	311	112	36.0	-89.0	303	216	71.3	-87.4	276	127	46.0	-89.1	276	127	46.0	-89.1
1000	301	116	38.5	-91.5	303	59	19.5	-91.2	300	86	28.7	-89.5	300	86	28.7	-89.5
1250	310	123	39.7	-90.4	301	71	23.6	-91.4	304	119	39.1	-90.1	304	119	39.1	-90.1
1500	310	151	48.7	-90.3	312	49	15.7	-91.4	296	72	24.3	-96.4	296	72	24.3	-96.4

RPM: rounds per minute; RSSI: received signal strength indicator.

**Figure 8.** Distribution of received packets as a heat map.**Figure 9.** The LoRa end device mounted to the (a) car's roof-rack and (b) boat's radio mast during coverage measurements.

The results of the experiment are summarized in Table 9. As one can notice, at reference points, the packet error rate was below 3%. Meanwhile, for the packets sent from the moving car, less than one-third of the packets were received properly. Figure 8 presents a heat map of the received packets. It illustrates that received packets are sufficiently distributed evenly over the entire motorway and thus this was not a persistent radio signal blockage which should have caused the packet losses. Furthermore, the results correlate well with the analysis and the angular velocity measurements.

Outdoor coverage

For characterizing the communication ranges and performance of the LoRa technology, the end device was attached to the roof-rack of the car (approximately at 2 m from the ground level, see Figure 9(a)) for on-ground measurement and to the radio mast of the boat for the measurements done in sea (see Figure 9(b)). The car was driven along the major roads at a speed of 40

Table 9. Results of the reference and the Doppler shift with car measurements.

Distance between end device and gateway (km)	Velocity of the car (km/h)	Relative velocity (km/h)	No. of transmitted packets	No. of received packets	Packet success ratio (%)
1.7 (reference point 1)	0	0	812	788	97.0
0.95 (reference point 2)	0	0	691	682	98.7
1.5 (reference point 3)	0	0	732	724	98.9
2.2 (reference point 4)	0	0	784	763	97.3
0.93–2.4	100	0–82.9	928	260	28.0

Table 10. Results of the coverage measurements done using car.

Range (km)	No. of transmitted packets	No. of received packets	Packet success ratio (%)
0–2	894	788	88
2–5	1215	1030	85
5–10	3898	2625	67
10–15	932	238	26
Total	6813	4506	66

Table 11. Results of the coverage measurements done using boat.

Range (km)	No. of transmitted packets	No. of received packets	Packet success ratio (%)
5–15	2998	2076	69
15–30	690	430	62
Total	3688	2506	68

to 100 km/h following the local speed limitations. The boat speed was around 5 knots (~ 9 km/h). The starting point for the on-water measurements was in the harbor located 5.1 km southwest from the gateway. The boat was driven outside and inside the harbor following the marked fairway.

The experiments were conducted in the city of Oulu, Finland, in spring and summer time in different weather conditions. The city is located on the shore of the Gulf of Bothnia (Baltic Sea) and has sufficiently flat landform. The area of the city is over 3000 km² with almost 200,000 inhabitants. The highest residential buildings are 10–12 floors, but most of the buildings in the city are 3–5 floors high. Tree forests mixed with farm land cover significant part of the suburban areas.

Tables 10 and 11 list the total number of transmitted packets by the end device, the number of packets received by the gateway and the packet loss ratio for the end device installed on the car and on the boat, respectively. Note that the total number of packets transmitted during the measurement campaign was around 10,000. Although this may be not sufficient for getting statistically reliable results, we expect that this number is still sufficient to draw the preliminary

conclusions about the capabilities of the LoRa technology.

A radio signal heat map of the Oulu region is presented in Figure 10. The map was built using Google Maps JavaScript API. The presented results reveal that within 2 km, the received signal is stronger than -100 dBm. Nonetheless, about 12% of the 894 transmitted packets were still lost. The possible reasons which may have caused this are the Doppler effect (see sections “Angular velocity” and “Linear velocity”), a line of sight blockade by various obstacles, and the interferences from other radio systems operating in the 868 MHz ISM band. In between 2 and 5 km range, the packet loss ratio does not increase significantly and remained below 15%. For the measurements made on the ground, the amount of radio packets lost from a distance of between 5 and 10 km was close to one-third. Finally, only a quarter of the packets sent from distances between 10 and 15 km were received correctly. Note that during the experiments we witnessed the delivery of the packets over more than 15 km, but communication at such distances is highly unreliable, at least when the end device is mobile. The most distant point for communication on water was almost 30 km

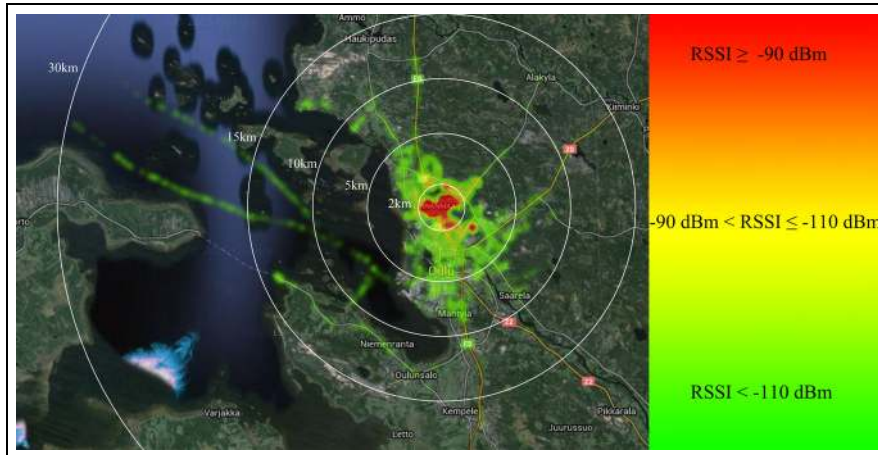


Figure 10. Received signal strength from different locations in Oulu, Finland, centered at the location of the base station (PTX = 14 dBm, GRX = 2 dBi, R = 293 bps, hTX = 2 m, and hRX = 24 m).

from the gateway. On water, in the range of 15–30 km, success rate was 62%.

Discussion

The LPWAN is an exciting new technology, which has a potential to become the wireless communication enabler for a variety of IoT applications. In this article, we focused on one of the perspective LPWAN technologies which is currently on the rise, named LoRa, and reported the results of a comprehensive analysis and the practical evaluation of the few key performance metrics of this technology.

First, to reveal the fundamentals of the LoRaWAN technology and the potential range of its applications, we analyzed the throughput of a LoRa link and the capacity of a LoRaWAN cell. The presented results show that in the best case, a single LoRa-enabled end device may upload the data with the rate of 1.8 kbps. For an application requiring transmission of only a single short packet per day, a single cell (featuring six LoRa 125 kHz, one LoRa 250 kHz, and one GFSK channels) may serve several millions of end devices. Accounting for the typical end device densities, a single gateway may cover an area of few kilometers in an urban zone and up to 30 km in a suburban zone. However, in case of end devices reporting every minute or so, only few thousands of end devices can reside in a single cell. Another factor limiting the scalability of the LoRaWAN solution is the distribution of the end devices within the cell, which is substantially uneven.

Second, in order to understand the feasibility of using LoRaWAN in the mobile applications, we analyzed and experimentally evaluated the performance of LoRa radio communication in the presence of Doppler shift. The results of the conducted analysis and measurement campaigns clearly show that for the LoRa

modulation with SF = 12 (which enables the longest communication range), when relative speed exceeds 40 km/h, the communication performance deteriorates. Meanwhile, under the low-speed mobility (i.e. below 25 km/h), the communication is still sufficiently reliable. This means that the LoRaWAN technology can be utilized for the variety of people- or animal-centric applications such as health and well-being monitoring, or tracking. It also worth noting that the lower SFs are expected to be less affected by the Doppler effect and thus may appear to be more suitable for mobile scenarios.

Third, to perceive the potential spatial lengths of the LoRaWAN communication links on one hand and assess the irreducible gateway densities on the other, we evaluated the coverage of the LoRaWAN. The coverage was measured by mounting the end device on the roof-rack of a car and on the radio mast of a boat and drove/sail around the gateway that is located at the University of Oulu, Finland. The gateway's antenna was located at a height of 24 m over the sea level. The LoRa end device was set to use transmit power of 14 dBm (25 mW), which provided for SF = 12 almost 30 km communication range with 62% of the packets delivered successfully within 15–30 km range on water. Within 2 and 5 km range on ground, 88% and 85% of the packets were successfully delivered, respectively. Note that some of the EU sub-bands enable the use of the transmit power exceeding 14 dBm, thus giving the possibility to increase the communication ranges even. To sum up, the presented results show that the LPWANs and the LoRaWAN technology, in particular, already today enable implementation of low-cost power-efficient long-range wireless communication. Due to these capabilities, the respective technologies can play an important role in enabling the variety of monitoring and actuating applications. Based on the

presented results, one can see that the targeted technologies can address rather well the needs and requirements of the traditional smart metering applications (e.g. gas, water, electricity, and garbage), civil engineering and road infrastructure monitoring (e.g. tunnels, bridges, and buildings), environment conditions (pollution and climate). Besides, LPWANs can be employed for tracking of vehicles (e.g. cars, bicycles, and motorcycles), as well as for monitoring the well-being of inhabitants.

Although the presented results shed some light on the important features and limitations of the LoRa technology, there are still many open questions which should be focused in future. First, in this research, we focused mainly and conducted our experiments using 125 kHz bandwidth LoRa signals with the maximum SF. In future, the other SFs, bandwidths, and modulation schemes need to be addressed as well. For this purpose, at a time, we are finalizing our own hardware LoRa end device design. Second, an important open problem is how well the technology will scale up in the real-life heterogeneous environment, given the different traffic patterns of the various applications and the potential interferences (both narrowband and wideband) from the other systems. Finally, the LoRaWAN is not the only LPWAN technology available today (one can consider the IEEE 802.15.4k, IEEE 802.15.4g, NB-IoT, and LTE-M, Sigfox, Weightless, and RPMA). The evaluation of their performance and the definition of the most advantageous applications for each of these technologies are also important. Also, the practical limitations have significantly limited us in the duration of our measurements. Even though the obtained results give some insight about the capabilities of the targeted technology, it would be interesting to extend the measurements covering different bandwidths, SFs, modulations, and environments.

Declaration of conflicting interests

The author(s) declared no potential conflicts of interest with respect to the research, authorship, and/or publication of this article.

Funding

The author(s) disclosed receipt of the following financial support for the research, authorship, and/or publication of this article: This work was partially funded by the Finnish Funding Agency for Innovation (Tekes) through VIRPA-C project.

References

1. Sigfox. <http://www.sigfox.com/en/> (accessed 9 August 2016).
2. LoRa Alliance. <https://www.lora-alliance.org/> (accessed 22 July 2016).
3. Weightless. <http://www.weightless.org/> (accessed 12 July 2016).
4. Weightless. Weightless-N open standard IoT networks deploy in Europe, <http://www.weightless.org/news/weightlessn-open-standard-iot-networks-deploy-in-europe> (accessed 15 June 2016).
5. Lauridsen M, Kovács IZ, Mogensen P, et al. Coverage and capacity analysis of LTE-M and NB-IoT in a rural area. In: *VTC workshop on cellular Internet of Things: emerging trends and enabling technologies*, Montreal, QC, Canada, 18–21 September 2016, pp.1–5. New York: IEEE.
6. Nokia. LTE-M—optimizing LTE for the Internet of Things, White paper, 2015, <https://novotech.com/docs/default-source/default-document-library/lte-m-optimizing-lte-for-the-internet-of-things.pdf?sfvrsn=0>
7. Hunn N. LoRa vs LTE-M vs Sigfox, <http://www.nic-khunn.com/lora-vs-lte-m-vs-sigfox/> (accessed 29 June 2016).
8. Sanchez-Iborra R and Cano M-D. State of the art in LPWAN solutions for industrial IoT services. *Sensors* 2016; 16: 708.
9. Nolan KE, Guibene W and Kelly MY. An evaluation of low power wide area network technologies for the Internet of Things. In: *2016 international wireless communications and mobile computing conference (IWCMC)*, Paphos, Cyprus, 5–9 September 2016, pp.439–444. New York: IEEE.
10. Reynders B, Meert W and Pollin S. Range and coexistence analysis of long range unlicensed communication. In: *23rd international conference on telecommunications (ICT)*, Thessaloniki, 16–18 May 2016, pp.1–6. New York: IEEE.
11. Petrić T, Goessens M, Nuaymi L, et al. Measurements, performance and analysis of LoRa FABIAN, a real-world implementation of LPWAN. In: *IEEE 27th annual international symposium on personal, indoor, and mobile radio communications (PIMRC)*, Valencia, 4–8 September 2016, pp.1–7. New York: IEEE.
12. Augustin A, Yi J, Clausen T, et al. A study of LoRa: long range & low power networks for the Internet of Things. *Sensors* 2016; 16: 1466.
13. Petäjajarvi J, Pettissalo M, Mikhaylov K, et al. On the coverage of LPWANs: range evaluation and channel attenuation model for LoRa technology. In: *14th international conference on intelligent transportation systems telecommunications (IIST)*, Copenhagen, 2–4 December 2015, pp.55–59. New York: IEEE.
14. Petäjajarvi J, Mikhaylov K, Hämäläinen M, et al. Evaluation of LoRa LPWAN technology for remote health and wellbeing monitoring. In: *10th international symposium on medical information and communication technology*, Worcester, MA, 20–23 March 2016, pp.1–5. New York: IEEE.
15. Mikhaylov K, Petäjajarvi J and Hänninen T. Analysis of capacity and scalability of the LoRa low power wide area network technology. In: *European wireless conference 2016 (EW16)*, Oulu, 18–20 May 2016, pp.1–6. Berlin: VDE-Verlag.

16. Wendt T, Volk F and Mackensen E. A benchmark survey of long range (LoRa™) spread-spectrum-communication at 2.45 GHz for safety applications. In: *16th annual wireless and microwave technology conference*, Cocoa Beach, FL, 13–15 April 2015, pp.1–4. New York: IEEE.
17. Semtech. LoRaWAN specification v1.0, January 2015, <https://www.lora-alliance.org/portals/0/specs/LoRaWAN%20Specification%201R0.pdf>
18. Semtech. *SX1272/3/6/7/8: LoRa modem design guide*. AN1200.13, Revision 1, July 2013, https://www.semtech.com/images/datasheet/LoraDesignGuide_STD.pdf
19. Semtech. *LoRa modulation basics*. AN1200.22, Revision 2, May 2015, <http://www.semtech.com/images/datasheet/an1200.22.pdf>
20. LoRa Alliance. A technical overview of LoRa and LoRaWAN. White paper, November 2015, <https://www.lora-alliance.org/portals/0/documents/whitepapers/LoRaWAN101.pdf>
21. Zhang P and Liu H. An ultra-wide band system with chirp spread spectrum transmission technique. In: *6th international conference on intelligent transportation systems telecommunications*, Chengdu, China, 21–23 June 2006, pp.294–297. New York: IEEE.
22. Rappaport TS. Mobile radio propagation: small-scale fading and multipath. In: *Wireless communications: principles and practice*, 1996, pp.139–196. New York: IEEE.
23. Semtech. *SX1272/73—860 MHz to 1020 MHz low power long range transceiver*. Datasheet, Revision 3, March 2015, <http://www.semtech.com/images/datasheet/sx1272.pdf> (accessed 11 August 2016).
24. Finnish Communications Regulatory Authority. *Regulation on collective frequencies for license-exempt radio transmitters and on their use*. 15AH/2015 M, February 2015, https://www.viestintavirasto.fi/attachments/maaraykset/Viestintavirasto15AH2015_en.pdf
25. IEEE 802.16 Broadband Wireless Access Working Group. Proposal for evaluation methodology for 802.16p—IEEE C802.16p-11/0102r2, Report, May 2011, <http://studylib.net/doc/17750736/ieee-c802.16n-11-0154-project-title>
26. Tanenbaum AS. The medium access sublayer. In: Camille Trentacoste (ed.) *Computer networks*. 3rd ed. Hoboken, NJ: Prentice Hall, 1996, pp.243–338.
27. Aref M and Sikora A. Free space measurements with Semtech LoRa technology. In: *Wireless systems within the conferences on intelligent data acquisition and advanced computing systems: technology and applications*, Offenburg, 11–12 September 2014, pp.19–23. New York: IEEE.
28. Aerial. Biconical antenna D100-1000, August 2014, http://aerial.fi/wp-content/uploads/2014/08/aerial_special.pdf (accessed 12 August 2016).
29. Semtech. *Planar F-antenna reference design*. AN1200.20, Revision 1, January 2014, http://www.semtech.com/images/datasheet/AN1200.20-SARANT_V1_0_STD.pdf